

# Sulfasalazine suppresses thyroid cancer cell proliferation and metastasis through T-cell originated protein kinase

LING ZOU<sup>1,2\*</sup>, ZHI GAO<sup>1\*</sup>, FANFAN ZENG<sup>2\*</sup>, JUANJUAN XIAO<sup>2</sup>, JUNMEI CHEN<sup>1</sup>,  
XIAOHONG FENG<sup>3</sup>, DI CHEN<sup>1</sup>, YING FANG<sup>1</sup>, JING CUI<sup>1</sup>, YANG LIU<sup>1</sup>,  
ZHI LI<sup>1</sup>, FENG ZHU<sup>2</sup>, QIUHONG DUAN<sup>2</sup> and XUAN LIN<sup>1</sup>

<sup>1</sup>Department of Internal Medicine, CR and WISCO General Hospital Affiliated to Wuhan University of Science and Technology, Wuhan, Hubei 430080; <sup>2</sup>Department of Biochemistry and Molecular Biology, School of Basic Medicine, Huazhong University of Science and Technology, Wuhan, Hubei 430030;

<sup>3</sup>Health and Family Planning Committee of Qingshan, Wuhan, Hubei 430080, P.R. China

Received October 21, 2018; Accepted June 25, 2019

DOI: 10.3892/ol.2019.10721

**Abstract.** Thyroid cancer patients with radioactive iodine-refractory or rapidly progressing presentation require effective treatment. T-cell originated protein kinase (TOPK) is highly expressed in a number of different tumor types, where it promotes proliferation and metastasis. However, the expression of TOPK in thyroid cancer is poorly documented. Therefore, immunohistochemistry was used to detect the expression of TOPK in thyroid cancer tissues, and its clinical significance in this disease was investigated. Sulfasalazine, a targeted inhibitor of TOPK that directly binds the protein with a dissociation constant (Kd) of 228  $\mu$ M, was also investigated using microscale thermophoresis. Sulfasalazine inhibited TOPK activity, as determined by an *in vitro* pull-down assay. Furthermore, sulfasalazine inhibited the proliferation and metastasis of thyroid cancer cells. The results indicated that TOPK may be a potential therapeutic target and diagnostic biomarker for thyroid cancer and may be used as an index to evaluate malignant thyroid nodules. Therefore, sulfasalazine is a potential novel compound for the targeted treatment of thyroid cancer.

## Introduction

Thyroid cancer is the most common of the endocrine malignancies (1). In developed countries, the age-standardized incidence of thyroid cancer is estimated to be 11.1 for every 100,000 females and 3.6 for every 100,000 males (2). This rate is reduced to 4.7 for females and 1.4 for males in developing countries (2). The most common type of thyroid cancer is papillary thyroid carcinoma (PTC), which accounts for 80% of all cases, followed by follicular thyroid cancer (FTC), which accounts for 10-20%. PTC and FTC are collectively referred to as differentiated thyroid carcinoma (DTC). In addition, medullary thyroid carcinoma (MTC) derived from parafollicular C cells comprises 5% of all thyroid cancer cases and exists in familial and sporadic forms (3). Anaplastic thyroid cancer (ATC) is one of the most aggressive and rapidly fatal types of thyroid cancer, which can evolve from DTC (4,5). The prognosis of DTC and MTC are relatively good, however, the prognosis of ATC is poor, in addition to its high potential for malignancy (6). Extreme variations in iodine intake, radiation exposure, sex hormones and environmental pollutants are risk factors for thyroid cancer (7,8). With continuously changing living environments and the wide application of high frequency ultrasound, the incidence of thyroid nodules is increasing annually (9). Among the clinically identified thyroid nodules, 5-15% are malignant (10), and the potential for metastasis is particularly high in young patients with Graves' disease (11,12). The increased mortality rate of thyroid cancer is also due to its high recurrence rate (13). Despite PTC being highly curable and presenting a good 10-year survival rate, 20-50% of patients are diagnosed with lymph node metastasis (14-16), and 5-20% of patients with total thyroidectomy have local recurrence (17,18). In addition, PTC may progress to poorly differentiated thyroid carcinomas or may completely lose differentiation and transform into ATC, which is prone to early metastasis and a poor prognosis (18).

The primary treatment for thyroid cancer includes surgery, radioactive iodine (RAI) and thyrotropin suppressive thyroid hormone therapy (4,19). Patients with RAI refractory, rapidly progressive or symptomatic disease require an effective

---

*Correspondence to:* Professor QiuHong Duan, Department of Biochemistry and Molecular Biology, School of Basic Medicine, Huazhong University of Science and Technology, 13 Hangkong Road, Qiaokou, Wuhan, Hubei 430030, P.R. China  
E-mail: duanqhwhz@hust.edu.cn

Dr Xuan Lin, Department of Internal Medicine, CR and WISCO General Hospital Affiliated to Wuhan University of Science and Technology, 29 Yejin Avenue, Qingshan, Wuhan, Hubei 430080, P.R. China  
E-mail: linxuan7777@126.com

\*Contributed equally

**Key words:** sulfasalazine, thyroid cancer, T-cell originated protein kinase, proliferation, metastasis

treatment (20). Until November 2013, the US Food and Drug Administration (FDA) recommended the use of doxorubicin in patients with ATC (21). However, owing to low and short-lived response rates, this treatment is now considered to be a poor option (22). Therefore, patients who develop RAI-refractory, rapidly progressive and/or symptomatic disease require additional treatment options. Targeted drugs are one such option; kinase inhibitor therapy may be used in patients with PTC and in patients for whom RAI is not suitable (23). Sorafenib is an oral multi-kinase inhibitor with targets including vascular endothelial growth factor receptor, rearranged during transfection (RET), B-type Raf (BRAF) and the receptor tyrosine kinase c-KIT (20). Lenvatinib and sorafenib are the two most recent, FDA-approved drugs for the treatment of RAI-refractory DTC (24), and the BRAF inhibitor vemurafenib is used to treat refractory PTC with BRAF mutation (25). However, due to drug toxicity and lack of durability, patients eventually stopped using aforementioned inhibitors (26). There is a requirement for new target molecules for the development of effective anticancer drugs.

T-cell originated protein kinase (TOPK), a serine/threonine protein kinase of the mitogen-activated protein kinase (MAPK) kinase family (27), was identified as a novel target for the treatment of thyroid cancer. PDZ-binding kinase (PBK)/TOPK expression was reportedly increased in highly proliferative malignant cells, but not in normal tissues (28,29), and therefore, TOPK overexpression may serve a key role in tumorigenesis and metastasis (29-31). A study by Matsuo *et al* (32) has suggested that the inhibition of TOPK is a feasible therapeutic option for the treatment of various human cancer types.

In the present study, the expression of TOPK in thyroid cancer tissues was identified by microarray, and its association with different types of thyroid cancer was discussed. In subsequent experiments, four thyroid cancer cell lines derived from different types of thyroid cancer were selected to detect the level of TOPK. Among all types of thyroid cancer, PTC is the most common histological type. Therefore, TOPK was overexpressed in a cell line derived from PTC (K1 cells) to explore the effect of altered TOPK expression on thyroid cancer. Subsequently, sulfasalazine was screened in an FDA-supported database as an inhibitor of TOPK. Sulfasalazine is an anti-inflammatory drug and has no known clinical application in anti-cancer therapy. Recently, a number of studies have confirmed that sulfasalazine also has anti-cancer properties against human tumors (33,34). However, little is known about the effects of sulfasalazine on thyroid cancer. The aim of the present study was to investigate whether sulfasalazine through TOPK suppresses thyroid cancer proliferation and metastasis. It is hoped that TOPK may be a novel biomarker and therapeutic target for the clinical diagnosis and treatment of thyroid cancer.

## Materials and methods

**Cell culture and transfection.** The human thyroid cancer cell lines SW579 (ATCC® HTB-107™) and TT (ATCC® CRL-1803™) were purchased from the American Type Culture Collection (ATCC). K1 cells and FTC133 cells were obtained from Guangzhou Cellcook Biotech Co., Ltd. The STR profiles obtained for the K1 cell in the present

study match the K1 STR profile provided by the European Collection of Authenticated Cell Cultures for those loci tested in common (Table SI). The SW579 cell line is derived from thyroid squamous cell carcinoma, a different type of thyroid cancer, TT cells are derived from MTC, K1 cells from PTC and the FTC133 cell line is derived from FTC.

K1, SW579, FTC133 and TT cells were cultured in DMEM, L-15, RPMI-1640 and F-12K media (Gibco; Thermo Fisher Scientific, Inc.), respectively, supplemented with 10% fetal bovine serum (FBS; Gibco; Thermo Fisher Scientific, Inc.). The cells were maintained at 37°C in a humidified atmosphere (5% CO<sub>2</sub>). The transfection reagent Simple-Fect was purchased from Signaling Dawn Biotech, and geneticin (G418) antibiotic was acquired from Sigma-Aldrich (Merck KGaA). The pcDNA3-HA-TOPK (8 µg) and empty pcDNA3 plasmid were transfected into K1 cells (80% confluency, 8x10<sup>6</sup> cells/10 cm<sup>2</sup> dish) according to the manufacturer's protocol. Sulfasalazine was purchased from Shanghai Zhongxi Three-dimensional Pharmaceutical Co., Ltd. and phenformin hydrochloride (PFH) from Jiangsu Yabang Epsen Pharmaceutical Co., Ltd.

**Western blotting.** Cells were harvested and lysed in radioimmunoprecipitation assay buffer [50 mM Tris (pH 7.4), 150 mM NaCl, 1 mM EDTA, 1 mM EGTA, 10 mg/ml aprotinin, 10 mg/ml leupeptin, 5 mM phenylmethanesulfonyl fluoride (PMSF), 1 mM dithiothreitol (DTT) and 1% Triton X-100]. The samples were sonicated 3 times on ice for 15 sec and centrifuged at 9,550 x g at 4°C for a further 15 min. The proteins were quantified using Bradford assay reagent (Bio-Rad Laboratories, Inc.), 40-60 µg separated using SDS-PAGE with a 10% gel and transferred to a PVDF membrane (EMD Millipore). The membranes were blocked with 5% non-fat milk or 5% BSA (BioSharp, Inc.) for 30 min at room temperature and incubated with primary antibody (Mouse anti-TOPK (cat. no., sc-393313; Santa Cruz Technology, Inc.; dilution, 1:1,000); anti-β-actin (cat. no., sc-47778; Cruz Technology, Inc.; dilution, 1:1,000) Anti-total-protein kinase B (T-AKT; cat. no., 9272s; Cell Signaling Technology, Inc.; dilution, 1:1,000), anti-phospho-AKT (p-AKT; S473; cat. no., 9271s; Cell Signaling Technology, Inc.; dilution, 1:500), anti-histone H3 XP rabbit monoclonal (mAb; cat. no., 4499; Cell Signaling Technology, Inc.; dilution, 1:1,000) and anti-phospho-histone H3 XP rabbit mAb (p-H3; cat. no., 3377s; Cell Signaling Technology, Inc.; dilution, 1:500) at 4°C overnight. The membranes were subsequently incubated with HRP-conjugated secondary antibody (Rabbit IgG; cat. no., E030120-2; dilution, 1:3,000; Mouse IgG; cat. no., E030110-02; dilution, 1:3,000; EarthOx Life) for 1 h at room temperature, and the protein bands were visualized using chemiluminescence (Bio-Rad Laboratories, Inc.). All experiments were repeated in triplicate.

**Thyroid cancer tissue microarray and immunohistochemical staining.** The thyroid carcinoma tissue arrays (cat. nos. BCC15014, TH961, TH641, TH242 and TH208) were purchased from Xi'an Elena Bio Co., Ltd. A total of 132 patients with thyroid cancer, including 44 males and 88 females, aged 20-86 years (median age, 48.43 years) provided samples for the tissue microarray; 56 tissues were from papillary carcinoma, 18 from follicular carcinoma,

Table I. Clinical characteristics of 132 patients with thyroid cancer.

		Stage			
Characteristics	Total	I	II	III	IV
Sex					
Female, n	88	25	26	21	16
Male, n	44	14	13	9	8
Sex ratio, F/M	2.0	1.79	2.0	2.33	2.0
Age, years					
Median	48.43	34.79	51.82	52.5	60
Range	20-86	20-71	20-77	32-79	39-86
Pathology					
PTC	56	31	13	9	3
FTC	18	4	5	5	4
MTC	42	4	21	16	1
ATC	16	0	0	0	16

PTC, papillary thyroid carcinoma; FTC, follicular thyroid cancer; MTC, medullary thyroid carcinoma; ATC, anaplastic thyroid cancer.

42 from medullary carcinoma and 16 from undifferentiated carcinoma. There were also 11 tissues from cases of thyroid adenoma, 18 normal thyroid tissue samples and 1 normal testicular tissue samples. Detailed information on patients is shown in Table I. The microarray tissues were deparaffinized in xylene and rehydrated in ethanol; high pressure repair with citrate buffer (pH 6.0) for 1.5 min was conducted, followed by endogenous peroxidase inactivation using hydrogen peroxide (0.3%) for 10 min at room temperature. The sections were washed 3 times with PBS and incubated with an anti-TOPK antibody (dilution, 1:200) at room temperature for 1 h. Biotin-labeled secondary antibody (DAKO; Agilent Technologies, Inc.; cat. no., K5007; dilution, 1:1,000) was added for 30 min at room temperature, and the sections were stained with 3,3'-diaminobenzidine, counterstained with hematoxylin for 5 min at room temperature, dehydrated and mounted. Positive staining was distinguished as brownish-yellow particles located in the cytoplasm and nuclei. A total of 10 high-power fields were randomly selected from each section and observed under a light microscope (magnification, x10). A total of 10 high-power fields were randomly selected from each section, and the scores were determined according to the staining intensity and percentage of positive cells. The hot-spot method was used for semi-quantification of immunohistochemical expression scores (35,36). Each case was evaluated by one observer and subsequently reviewed by another observer using the semi-quantitative classifications proposed by Yuan *et al* (35) and Montgomery *et al* (36). The semi-quantified positive expression index (PEI, 0-12) of TOPK was calculated based on the percentage of positivity of tumor cells (1, 0-25%; 2, 26-50%; 3, 51-75%; and 4, 76-100%), staining intensity score (0, none; 1, weak; 2, moderate; 3, intense), and an overall score (0-12) calculated for each case by multiplying percentage score with intensity score.

**MTT assay.** To estimate cell viability,  $5 \times 10^3$  cells/well were seeded in 96-well plates and cultured for 24, 48, 72 and 96 h. MTT was added to each well, and the cells were incubated for 4 h at 37°C. Following incubation, the formazan crystals were dissolved in 150 ml dimethyl sulfoxide, and absorbance was determined at a wavelength of 490 nm within 10 min. To assess sulfasalazine inhibition,  $5 \times 10^3$  cells/well were seeded in 96-well plates and cultured for 24 h; fresh medium containing different concentrations of sulfasalazine was applied, and cells were cultured for a further 72 h. Sulfasalazine cytotoxicity was measured using an MTT assay as described above. The experiments were performed in triplicate, and the mean absorbance values were calculated with non-treated cells as the negative control.

**Anchorage-independent growth assay (soft agar assay).** A total of  $1 \times 10^4$  cells/well were seeded in a 6-well plate; sample cells were treated with different concentrations of sulfasalazine, while control cells were left untreated. The cells were cultured in 1 ml Basal Medium Eagle agar (0.33%; Sigma-Aldrich; Merck KGaA) containing 10% FBS, 2 mM L-glutamine and 25 µg/ml gentamicin, maintained at 37°C (5% CO<sub>2</sub>) for 5-10 days. Analysis of the resultant colonies under a white light, 4x microscope.

**Wound healing assay.** Stable cell lines were grown in 6-well plates and serum-starved overnight. To create a wound, the cell monolayer was scraped using a sterile pipette tip. The cells were washed with media and incubated in growth medium with or without inhibitors for 0, 24, 30 or 36 h. The cells were imaged under a light microscope (magnification, x10), and each assay was repeated at least three times.

**In vitro kinase assay.** Active TOPK (EMD Millipore) phosphorylates and subsequently activates its downstream substrate histone H3. Active TOPK (0.2 mg) was incubated with sulfasalazine in 1X kinase buffer [25 mM Tris-HCl (pH 7.5), 5 mM β-glycerophosphate, 2 mM DTT, 0.1 mM Na<sub>3</sub>VO<sub>4</sub>, 10 mM MgCl<sub>2</sub> and 5 mM MnCl<sub>2</sub>] at 32°C for 20 min. Inactive histone H3 (4 µg) and 100 µM ATP were added and the reaction was incubated at 32°C for 1.5 h. The reactions were treated with 5X SDS sample buffer and analyzed by western blotting, as aforementioned.

**Microscale thermophoresis.** Recombinant TOPK was labeled with the Monolith NT™ Protein Labeling Kit RED (NanoTemper Technologies GmbH) according to the manufacturer's protocol. His tag labeled TOPK was used at 250 nM. The samples were diluted in 20 mM HEPES (pH 7.4) supplemented with 0.05% (v/v) Tween-20. Sulfasalazine was dissolved in 0.4% NaHCO<sub>3</sub> to a concentration of 50 mM and serially diluted from a starting concentration of 4 mM. Samples were incubated for 10 min at room temperature, and loaded into Monolith NT standard-treated capillaries; thermophoresis was measured at 25°C following a 30 min incubation on a Monolith NT.115 instrument (NanoTemper Technologies GmbH). The laser power was set to 20 or 40%, with 30 sec 'on'-time, and an LED power of 100%. The dissociation constant (K<sub>d</sub>) was distinguished using NTA software (NanoTemper Technologies GmbH) (37).

**In vitro pull-down assay.** Sulfasalazine-conjugated and un-conjugated Sepharose® 4B beads were prepared as previously reported (38). The Sepharose beads were incubated with His tag labeled recombinant TOPK protein in reaction buffer [50 mM Tris-HCl (pH 7.5), 5 mM EDTA, 150 mM NaCl, 1 mM DTT, 0.01% NP-40, 2 µg/ml BSA, 0.02 mM PMSF and 1 µg/ml protease inhibitor cocktail (Roche Applied Science)] with gentle rotation at 4°C overnight. The beads were subsequently rinsed 5 times in wash buffer [50 mM Tris-HCl (pH 7.5), 5 mM EDTA, 150 mM NaCl, 1 mM DTT, 0.01% NP-40 and 0.02 mM PMSF], and the bead-bound proteins were analyzed using western blotting with an anti-TOPK antibody, as aforementioned.

**Homology modeling and molecular docking.** The crystal structure of IRAK-4 kinase (PDB code: 2NRU) was used as a template, and the homology model of human TOPK (Accession No.: NP\_060962) was used with MODELLER, an automated homology modeling program (39,40). The subset zdd (ZINC Drug Database), which includes all commercially approved drugs and nutraceuticals worldwide, was downloaded as input from the ZINC as a docking input for the mol2 file (41). Docking was performed on the Intel i7 4960 using the ICM 3.8.1 modeling software processor (MolSoft L.L.C.) (42). Ligands that bind pocket residues were selected using graphical tools in ICM software, to create a boundary docking search. In docking calculations, the potential energy map of the receptor is calculated using default parameters. These compounds are imported into ICM and an index file is created. Conformation sampling is based on the Monte Carlo program, and finally the lowest energy and the most favorable orientation ligands were selected.

**Statistical analysis.** Clinical statistical analysis (Tables II and III) was conducted using SPSS version 13.0 software (SPSS Inc.), and the data were compared by  $\chi^2$  analysis. All other statistical analyses were performed using GraphPad Prism 7.0 software (GraphPad Software, Inc.). Analysis of multiple groups was performed using one-way ANOVA and Tukey's post hoc test. Student's t-test was used to compared between two groups. All data are presented as the mean  $\pm$  standard deviation, and  $P < 0.05$  was considered to indicate a statistically significant difference.

## Results

*TOPK is upregulated in thyroid carcinoma tissues and may be used as an evaluation index for malignant thyroid nodules.* The expression level of TOPK was established in 132 thyroid cancer, 11 thyroid adenoma and 18 normal thyroid samples, and 1 testicular tissue sample using immunohistochemistry (Fig. 1). Expression levels of TOPK were scored from 0 to 12 according the definition described in the materials and methods section. PEI of 7-12 of TOPK for well-differentiated thyroid cancer (DTC) was 37.84%, and that for poorly differentiated thyroid cancer (MTC and ATC) was 68.97%, as presented in in Table II. There was a significant association between the pathological types of thyroid cancer and the intensity of TOPK ( $P < 0.001$ ). For thyroid cancer clinical stages I-II, PEI of 7-12 for TOPK is 43.59%, and that for clinical stages III-IV

Table II. PEI of T-cell originated protein kinase in different types of thyroid cancer.

PEI	DTC (PTC and FTC), n (%)	MTC and ATC, n (%)
0-6	46 (62.16)	18 (31.03)
7-12	28 (37.84)	40 (68.97)

PEI, positive expression index; DTC, differentiated thyroid carcinoma; PTC, papillary thyroid carcinoma; FTC, follicular thyroid cancer; MTC, medullary thyroid carcinoma; ATC, anaplastic thyroid cancer. Pearson  $\chi^2$  results:  $\chi^2 = 12.614$ ,  $P < 0.001$ .

Table III. PEI of T-cell originated protein kinase at different stages of thyroid cancer.

PEI	I and II, n (%)	III and IV, n (%)
0-6	44 (56.41)	20 (37.04)
7-12	34 (43.59)	34 (62.96)

PEI, positive expression index. Pearson  $\chi^2$  results:  $\chi^2 = 4.795$ ,  $P = 0.029$ .

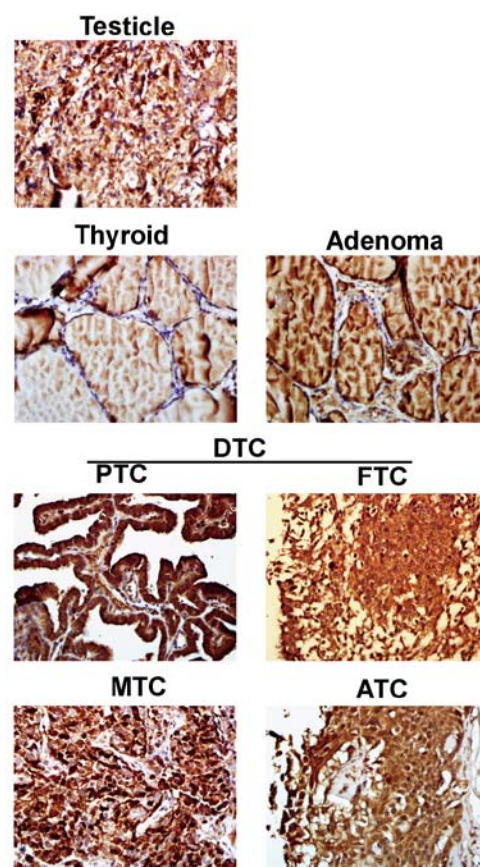


Figure 1. TOPK is overexpressed in thyroid carcinoma tissues and may be used as an index to evaluate malignancy in thyroid nodules. Immunohistochemical examination of TOPK expression. Images are from a single representative case. TOPK, T-cell originated protein kinase; DTC, differentiated thyroid carcinoma; MTC, medullary thyroid carcinoma; ATC, anaplastic thyroid cancer; PTC, papillary thyroid carcinoma; FTC, follicular thyroid cancer.



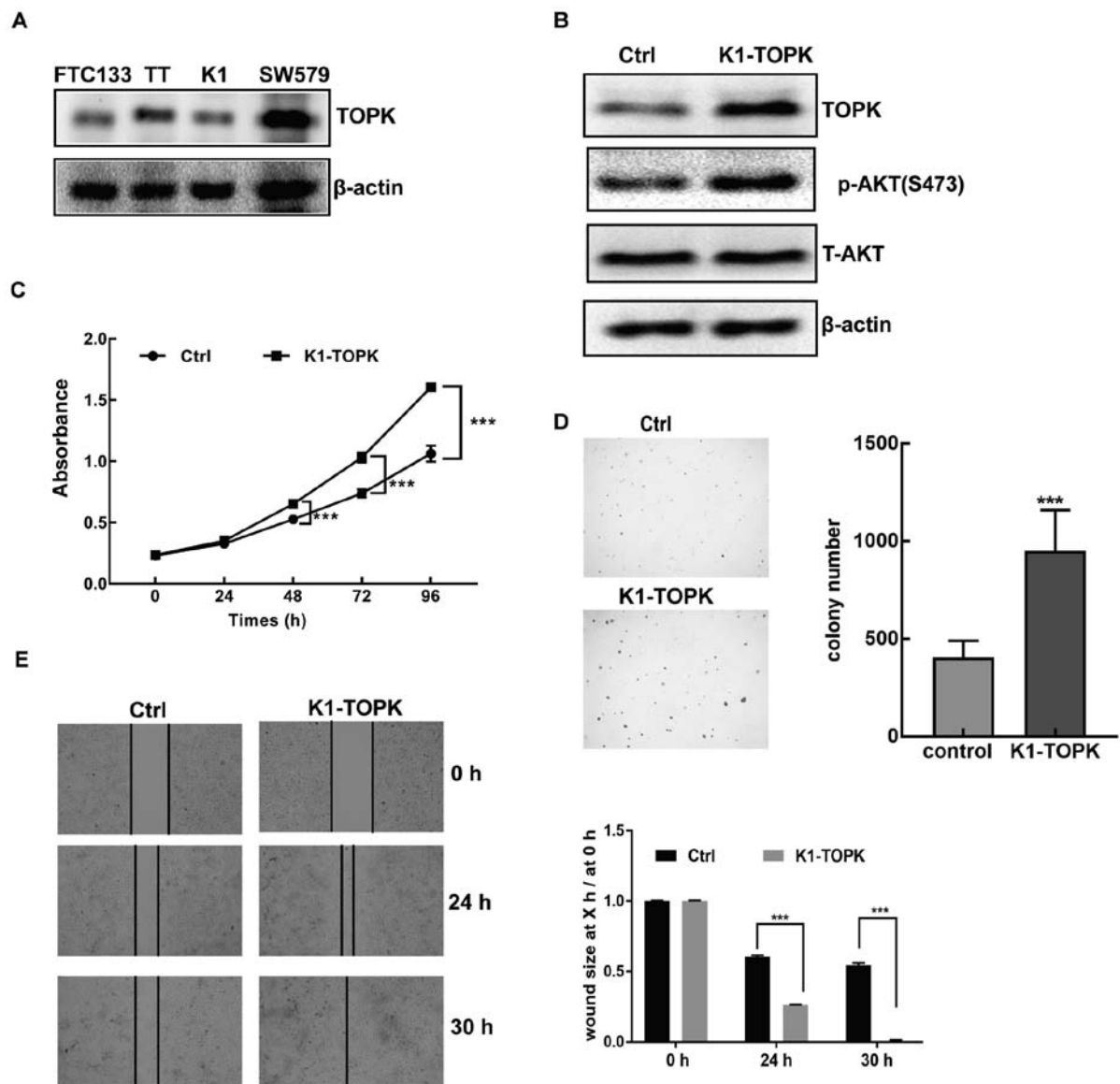


Figure 2. TOPK overexpression promotes the proliferation and metastasis of thyroid cancer cells. (A) Protein expression of TOPK in FTC133, TT, K1 and SW579 thyroid cancer cell lines analyzed using western blotting. (B) Protein expression of TOPK, p-AKT and AKT in K1-TOPK cells. (C) Absorbance rate (nm) of K1-TOPK cells, as determined by MTT assay. (D) Colony formation and (E) migration of K1-TOPK cells assessed using soft agar and wound-healing assays, respectively. Data are represented as the mean  $\pm$  standard deviation from triplicate experiments. \*\*\* $P < 0.001$ . TOPK, T-cell originated protein kinase; p-AKT, phosphorylated protein kinase B; T-AKT, total protein kinase B; Ctrl, control.

is 62.96% shown in Table III. The present results identified a significant association between TOPK expression and clinical stage of thyroid carcinoma ( $P = 0.026$ ). These results indicated that the high expression level of TOPK in patients with thyroid carcinoma is associated with pathological type and clinical stage of disease. This suggests that TOPK may be used as an index to evaluate malignant thyroid nodules.

*TOPK overexpression promotes the proliferation and metastasis of thyroid cancer cells.* The expression levels of TOPK were determined in different thyroid cancer cell lines (K1, SW579, TT and FTC133 cells), and the results revealed that TOPK expression level was lowest in K1 cells derived from a metastasis of PTC (Fig. 2A). PTC is the most common type of thyroid cancer, and therefore, the effects of TOPK-overexpression in K1 cells were investigated. A stable

cell line overexpressing TOPK (K1-TOPK) was established to observe the effects on proliferation and metastasis of PTC-derived cells (Fig. 2B). TOPK overexpression significantly increased the proliferation of K1-TOPK cells compared with control cells (Fig. 2C;  $P < 0.001$ ). Anchorage-independent growth is a hallmark of *in vitro* transformed and cancer cells, thus anchorage-independent colony formation ability was assessed using a soft agar assay. The number and size of the colonies formed by K1-TOPK cells was greater compared with those of the control group (Fig. 2D) indicating that increased TOPK expression may promote thyroid cancer cell proliferation. TOPK promotion of metastasis in thyroid cancer cells was also assessed using a wound-healing assay, in which the overexpression of TOPK resulted in a marked increase in cell migration ( $P < 0.001$ ; Fig. 2E). A previous study confirmed that TOPK is involved in the MAPK pathway, and that this

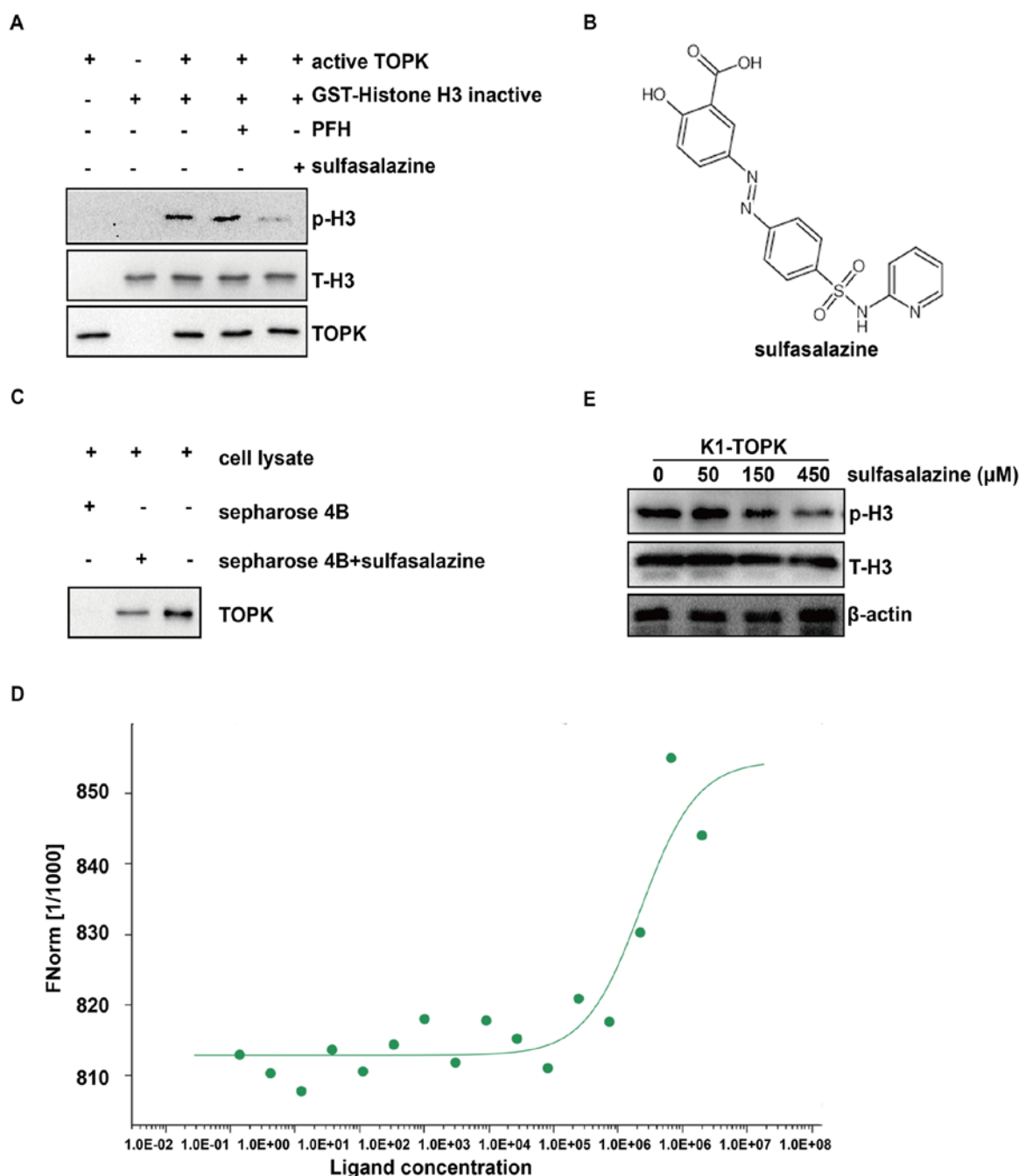


Figure 3. Sulfasalazine directly binds TOPK and inhibits its activity *in vitro*. (A) Inhibitory effect of sulfasalazine on TOPK activity was determined using an *in vitro* kinase assay and subsequent western blot analysis. (B) Chemical structure of sulfasalazine. (C) *In vitro* pull-down assay was performed to detect sulfasalazine binding to TOPK. (D) Affinity between sulfasalazine and TOPK was determined using microscale thermophoresis;  $K_D$ =228  $\mu$ M. (E) Sulfasalazine decreased the level of p-H3 (Ser10) in a dose-dependent manner, as determined by western blot analysis. Data are representative of 3 experiments. TOPK, T-cell originated protein kinase; PFH, phenformin hydrochloride; p-H3, phosphorylated histone H3; T-H3, total-histone H3.

enhances cell migration by modulating PI3K/PTEN/AKT signaling (28). The MAPK and PI3K/AKT pathways are associated with molecular pathogenesis in thyroid cancer (43) and as such, the level of p-AKT was detected in K1-TOPK cells. The results demonstrated that the level of p-AKT in K1-TOPK cells was higher compared with that of the control cells (Fig. 2B), indicating that TOPK promotes the activation of AKT signaling.

*Sulfasalazine directly binds TOPK and inhibits its activity in vitro.* The results of the present study suggest that TOPK

may be an important target for the treatment of thyroid cancer; however, there are currently no compounds in clinical use that directly target TOPK. Using homologous modeling, potential TOPK inhibitors were screened in an FDA-supported database, and sulfasalazine and PFH were selected for further analysis. An *in vitro* kinase assay was performed using histone H3 as a substrate, and the results demonstrated that sulfasalazine inhibited TOPK activity (Fig. 3A). The data revealed that phosphorylation of histone H3 (Ser10) was substantially attenuated following treatment with sulfasalazine, but not PFH (Fig. 3A), suggesting that sulfasalazine is a potential inhibitor of TOPK.

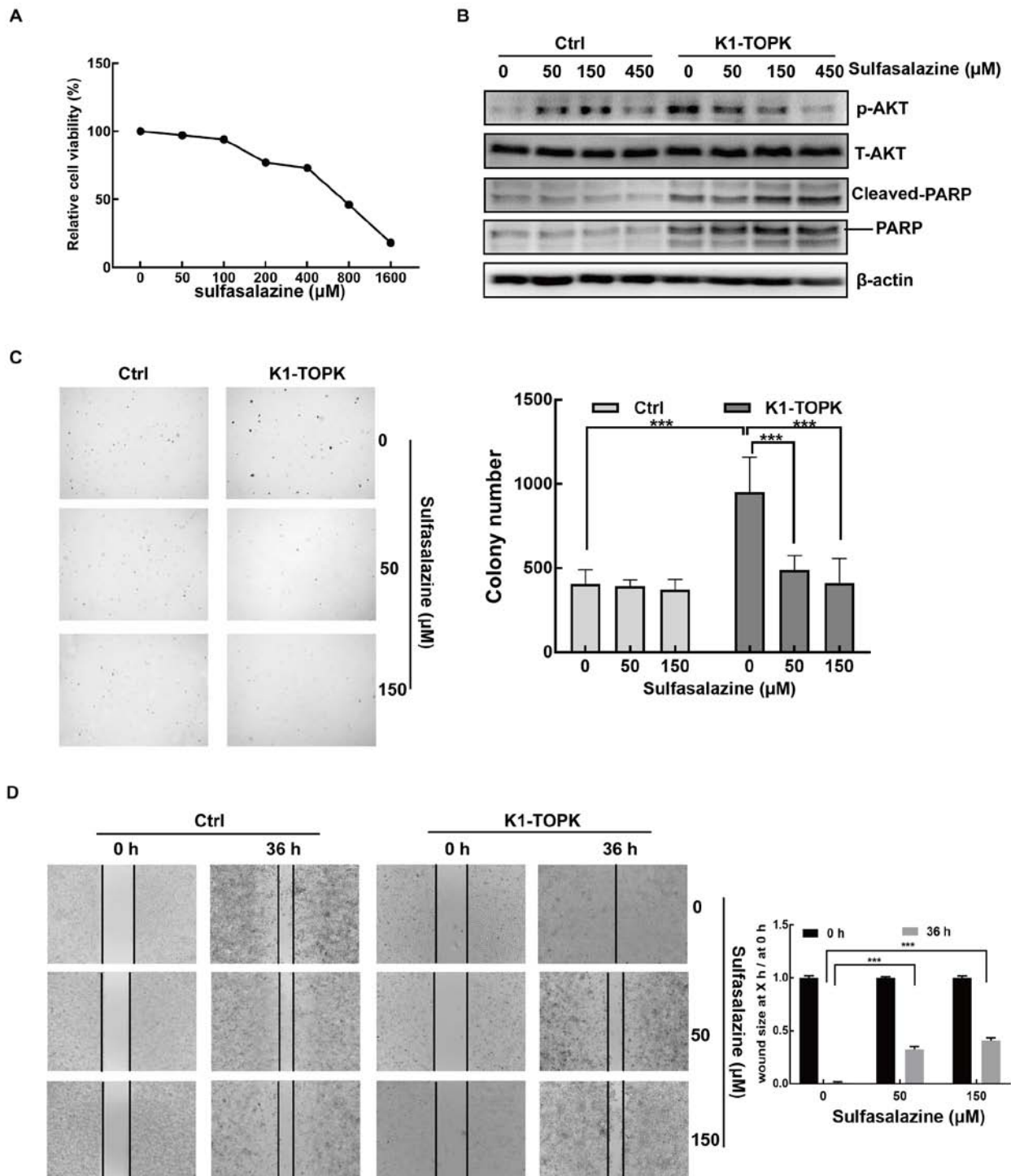


Figure 4. Sulfasalazine targeting of TOPK inhibits the proliferation and metastasis of TOPK-overexpressing thyroid cancer cells. (A) Viability of K1 cells following treatment with sulfasalazine for 72 h analyzed using an MTT assay. (B) Sulfasalazine decreased the level of p-AKT in K1-TOPK cells in dose-dependent manner. The level of cleaved-PARP was increased by sulfasalazine in a dose-dependent manner. (C) Sulfasalazine inhibited the anchorage-independent growth and (D) motility of K1-TOPK cells, as determined using colony formation and wound-healing assays. \*\*\* $P < 0.001$ . TOPK, T-cell originated protein kinase; p-AKT, phosphorylated protein kinase B; T-AKT, total protein kinase B; PARP, poly (ADP-ribose) polymerase; Ctrl, control.

The molecular structure of sulfasalazine is presented in Fig. 3B. In addition, an *in vitro* pull-down assay was performed to detect the potential interaction between TOPK and sulfasalazine. TOPK was detected in the sample eluent from Sepharose 4B beads coupled with sulfasalazine, but not in the eluent from Sepharose beads alone, indicating that sulfasalazine directly binds TOPK (Fig. 3C). Furthermore, the affinity of TOPK for

sulfasalazine was assessed using microscale thermophoresis, revealing a  $K_d$  of 228  $\mu\text{M}$  (Fig. 3D). Using the stable cell line K1-TOPK, phosphorylation of histone H3 was significantly reduced in a dose-dependent manner following treatment with sulfasalazine, indicating that it may act as an inhibitor of TOPK in thyroid cancer cells (Fig. 3E). Thus, sulfasalazine can interact with TOPK and inhibit its activity *in vitro*.

*Sulfasalazine inhibits the proliferation and metastasis of TOPK-overexpressing thyroid cancer cells.* As an inhibitor of TOPK, the antiproliferative and antimetastatic properties of sulfasalazine in thyroid cancer were further investigated. The cytotoxicity of sulfasalazine was assessed in K1 cells; cells were treated with increasing concentrations of sulfasalazine for 72 h, and cell viability was measured using an MTT assay. The results indicated K1 cell viability was 73% when treated with sulfasalazine at a concentration of 400  $\mu$ M. (Fig. 4A). The expression levels of p-AKT in K1-TOPK cells and control cells were also determined. The level of p-AKT in K1-TOPK cells decreased with increasing concentrations of sulfasalazine (Fig. 4B), but in control group cells appears to be increased treated with sulfasalazine at 50 and 150  $\mu$ M, and reduced at 450  $\mu$ M. Additionally, the level of cleaved-PARP increased with increasing concentrations of sulfasalazine in K1-TOPK cells (Fig. 4B), suggesting that sulfasalazine induced apoptosis.

The effects of sulfasalazine on anchorage-independent colony formation ability were also investigated. The results revealed that K1-TOPK cells treated with sulfasalazine formed fewer colonies compared with untreated K1-TOPK cells (Fig. 4C;  $P < 0.001$ ), and that sulfasalazine may attenuate anchorage-independent cell growth. In addition, the effect of sulfasalazine on thyroid cancer cell metastasis was observed using a wound healing assay. The results presented in Fig. 4D demonstrate that at 36 h post treatment, sulfasalazine significantly inhibited the migration of K1-TOPK cells ( $P < 0.001$ ). Collectively, the results suggest that sulfasalazine-targeting of TOPK inhibits the proliferation and metastasis of thyroid cancer cells.

## Discussion

The five-year survival rate of patients with thyroid cancer differs with cancer stage; the five-year survival rate is 59% in the later stages, whilst the early localized stage is closer to 100% (44). Therefore, early diagnosis is necessary to reduce mortality rate. Currently, the most reliable and cost-effective diagnostic method for the detection of thyroid nodules is guided fine needle aspiration (FNA) and cytological evaluation of tissues (10). FNA cytology has a high level of accuracy and specificity; however, 10-40% of FNA samples are diagnosed as indeterminate malignancies (45,46). Molecular markers may improve tumor diagnostic sensitivity, as 60-70% of thyroid cancers harbor at least one known genetic mutation (47,48). Currently, molecular diagnostic markers for thyroid cancer are BRAF and RAS mutations, and RET rearranged in PTC and paired box gene 8/peroxisome proliferator-activated receptor  $\gamma$ 1 gene rearrangements (49). Molecular testing has improved the detection of malignancy in indeterminate cytological nodules; the probability of malignancy among these nodules is 40%, though mutation-positive nodules are invariably malignant, and 16% of cytological nodules are mutation-negative (48). Furthermore, the aforementioned diagnostic markers have limited sensitivity (50) as they fail to adequately exclude cancer within suspicious nodules, which may result in unnecessary surgery. ATC has a high degree of malignancy and poor prognosis (51). This suggests that TOPK may be a prognostic indicator for thyroid cancer, and may be

used as a diagnostic marker to evaluate malignant thyroid nodules in early diagnosis.

TOPK is a potential therapeutic target and is highly expressed in various malignancies, including breast cancer, colorectal cancer, prostate cancer, lung cancer and lymphoma (32). It is also necessary for cancer cell mitosis (52). In breast cancer, histone H3 phosphorylation (Ser10) by PBK/TOPK was demonstrated *in vitro* and *in vivo*, suggesting that the kinase activity of TOPK may be involved in its oncogenic function (53). In colorectal cancer, the positive feedback loop between TOPK and MAPK1 increased tumorigenesis, indicating that TOPK-regulated signaling may serve as a potential therapeutic target (54). Association between high levels of TOPK and an advanced grade of cancer, metastasis and invasiveness have previously been identified in prostate cancer (55,56). Therefore, TOPK may perform an oncogenic cellular function by promoting tumor cell growth, proliferation, differentiation, migration and/or invasion. These findings suggest that TOPK may be a potential drug target for cancer therapy. However, there are no treatments in clinical use that specifically target TOPK. There are currently two TOPK inhibitors, HI-TOPK-032 (57) and OTS964 (58); yet due to the unfavorable solubility and toxicity of these compounds, they are unsuitable for clinical use at this time. The development of novel compounds is further hindered by the high cost and low success rate of clinical trials, and the difficulty in transitioning from preclinical screening.

Drug re-use, the use of existing drugs for new applications, is a less expensive option and allows for faster progress to clinical trial stage (59). In the present study, homologous modeling was employed to screen an FDA-approved drug database, and sulfasalazine was identified as a TOPK inhibitor. Sulfasalazine was found to inhibit proliferation and metastasis of thyroid cancer at a low concentration, potentially by targeting TOPK. A number of studies demonstrated that PBK/TOPK knockdown resulted in cell cycle arrest at the G<sub>2</sub>/M phase, and significantly decreased CDC2 and cyclin B expression (60). The present study revealed that sulfasalazine directly bound TOPK and inhibited its activity *in vitro*. Therefore, although the present study demonstrated that sulfasalazine induced apoptosis, this compound may affect the cell cycle by targeting TOPK which will be validated by flow cytometry in future studies. Previous studies have confirmed that TOPK promotes the proliferation and migration of tumor cells by modulating the PTEN/AKT-dependent signaling pathways (28,61), and that the PI3KCA/AKT pathways are associated with the molecular pathogenesis of thyroid cancer (43). In the present study, sulfasalazine reduced the level of p-AKT in a dose-dependent manner. Therefore, sulfasalazine targets TOPK and influences the PI3K/AKT signaling pathway. Although sulfasalazine is already in clinical use, clinical trials are needed to assess its inhibitory effects and potential toxicity in thyroid cancer.

In conclusion, TOPK may be used as an evaluation index for malignant thyroid nodules and may be a novel therapeutic target. Due to its inhibitory activity towards TOPK, sulfasalazine may be a potential target drug for the effective management of thyroid cancer.



## Acknowledgements

The authors would like to acknowledge Dr Hui Lu, Dr Qing Tian, Dr Ping Yuan and Dr Lin Liu (Department of Biochemistry and Molecular Biology, School of Basic Medicine, Huazhong University of Science and Technology) for offering advice on the manuscript.

## Funding

This project was supported by the National Natural Science Foundation of China (grant nos. 81672936, 81672739 and 81472602), the Independent Innovation Project of Huazhong University of Science and Technology (grant nos. 2016YXZD034 and 2015QN151) and the Health and Family Planning Commission of Hubei Province (grant no. WJ2017M207).

## Availability of data and materials

The datasets used and/or analyzed during the current study are available from the corresponding author on reasonable request.

## Authors' contributions

LZ, ZG, FZ participated in the experiments. XL purchased the chip. XL, ZG and FZ analyzed the tissue samples. JX, JC, XF, DC, YF, JC, YL, ZL performed the immunohistochemistry experiment and statistical analysis. LZ, FZ and QD designed experiments, analyzed data and drafted the manuscript. All authors read and approved the final manuscript.

## Ethics approval and consent to participate

Not applicable.

## Patient consent for publication

Not applicable.

## Competing interests

The authors declare that they have no competing intetests.

## References

- Wiltshire JJ, Drake TM, Uttley L and Balasubramanian SP: Systematic review of trends in the incidence rates of thyroid cancer. *Thyroid* 26: 1541-1552, 2016.
- Torre LA, Bray F, Siegel RL, Ferlay J, Lortet-Tieulent J and Jemal A: Global cancer statistics, 2012. *CA Cancer J Clin* 65: 87-108, 2015.
- Song H, Lin C, Yao E, Zhang K, Li X, Wu Q and Chuang PT: Selective ablation of tumor suppressors in Parafollicular C cells elicits medullary thyroid carcinoma. *J Biol Chem* 292: 3888-3899, 2017.
- Haugen BR, Alexander EK, Bible KC, Doherty GM, Mandel SJ, Nikiforov YE, Pacini F, Randolph GW, Sawka AM, Schlumberger M, *et al*: 2015 American Thyroid Association Management Guidelines for adult patients with thyroid nodules and differentiated thyroid cancer: The American Thyroid Association Guidelines Task Force on thyroid nodules and differentiated thyroid cancer. *Thyroid* 26: 1-133, 2016.
- Zarebczan B and Chen H: Multi-targeted approach in the treatment of thyroid cancer. *Minerva Chir* 65: 59-69, 2010.
- Burman KD: Is poorly differentiated thyroid cancer poorly characterized? *J Clin Endocrinol Metab* 99: 1167-1169, 2014.
- de Vathaire F, Haddy N, Allodji RS, Hawkins M, Guibout C, El-Fayech C, Teinturier C, Oberlin O, Pacquement H, Diop F, *et al*: Thyroid radiation dose and other risk factors of thyroid carcinoma following childhood cancer. *J Clin Endocrinol Metab* 100: 4282-4290, 2015.
- Vigneri R, Malandrino P, Giani F, Russo M and Vigneri P: Heavy metals in the volcanic environment and thyroid cancer. *Mol Cell Endocrinol* 457: 73-80, 2017.
- Zevallos JP, Hartman CM, Kramer JR, Sturgis EM and Chiao EY: Increased thyroid cancer incidence corresponds to increased use of thyroid ultrasound and fine-needle aspiration: A study of the Veterans Affairs health care system. *Cancer* 121: 741-746, 2015.
- American Thyroid Association (ATA) Guidelines Taskforce on Thyroid Nodules and Differentiated Thyroid Cancer; Cooper DS, Doherty GM, Haugen BR, Kloos RT, Lee SL, Mandel SJ, Mazzaferri EL, McIver B, Pacini F, *et al*: Revised American Thyroid Association management guidelines for patients with thyroid nodules and differentiated thyroid cancer. *Thyroid* 19: 1167-1214, 2009.
- Ren M, Wu MC, Shang CZ, Wang XY, Zhang JL, Cheng H, Xu MT and Yan L: Predictive factors of thyroid cancer in patients with Graves' disease. *World J Surg* 38: 80-87, 2014.
- Tassinari J and Sisti A: Exophthalmos (Graves' orbitopathy) in an ancient sculpture. *J Endocrinol Invest* 39: 1085-1086, 2016.
- Smallridge RC, Ain KB, Asa SL, Bible KC, Brierley JD, Burman KD, Kebebew E, Lee NY, Nikiforov YE, Rosenthal MS, *et al*: American Thyroid Association guidelines for management of patients with anaplastic thyroid cancer. *Thyroid* 22: 1104-1139, 2012.
- Lee YS, Lim H, Chang HS and Park CS: Papillary thyroid microcarcinomas are different from latent papillary thyroid carcinomas at autopsy. *J Korean Med Sci* 29: 676-679, 2014.
- Donatini G, Castagnet M, Desurmont T, Rudolph N, Othman D and Kraimps JL: Partial thyroidectomy for papillary thyroid microcarcinoma: Is completion total thyroidectomy indicated? *World J Surg* 40: 510-515, 2016.
- Goldfarb M and Casillas J: Unmet information and support needs in newly diagnosed thyroid cancer: Comparison of adolescents/young adults (AYA) and older patients. *J Cancer Surviv* 8: 394-401, 2014.
- Grant CS: Papillary thyroid cancer: Strategies for optimal individualized surgical management. *Clin Ther* 36: 1117-1126, 2014.
- Zhu W, Zhong M and Ai Z: Systematic evaluation of prophylactic neck dissection for the treatment of papillary thyroid carcinoma. *Jpn J Clin Oncol* 43: 883-888, 2013.
- Wells SA Jr, Asa SL, Dralle H, Elisei R, Evans DB, Gagel RF, Lee N, Machens A, Moley JF, Pacini F, *et al*: Revised American Thyroid Association guidelines for the management of medullary thyroid carcinoma. *Thyroid* 25: 567-610, 2015.
- Dadu R, Devine C, Hernandez M, Waguespack SG, Busaidy NL, Hu MI, Jimenez C, Habra MA, Sellin RV, Ying AK, *et al*: Role of salvage targeted therapy in differentiated thyroid cancer patients who failed first-line sorafenib. *J Clin Endocrinol Metab* 99: 2086-2094, 2014.
- Schlumberger M, Parmentier C, Delisle MJ, Couette JE, Droz JP and Sarrazin D: Combination therapy for anaplastic giant cell thyroid carcinoma. *Cancer* 67: 564-566, 1991.
- Tennvall J, Lundell G, Wahlberg P, Bergenfelz A, Grimelius L, Akerman M, Hjelm Skog AL and Wallin G: Anaplastic thyroid carcinoma: Three protocols combining doxorubicin, hyperfractionated radiotherapy and surgery. *Br J Cancer* 86: 1848-1853, 2002.
- Tuttle RM, Haddad RI, Ball DW, Byrd D, Dickson P, Duh QY, Ehya H, Haymart M, Hoh C, Hunt JP, *et al*: Thyroid carcinoma, version 2.2014. *J Natl Compr Canc Netw* 12: 1671-1680.
- Wilson L, Huang W, Chen L, Ting J and Cao V: Cost effectiveness of Lenvatinib, Sorafenib and placebo in treatment of radioiodine-refractory differentiated thyroid cancer. *Thyroid* 27: 1043-1052, 2017.
- Flaherty KT, Puzanov I, Kim KB, Ribas A, McArthur GA, Sosman JA, O'Dwyer PJ, Lee RJ, Grippo JF, Nolop K and Chapman PB: Inhibition of mutated, activated BRAF in metastatic melanoma. *N Engl J Med* 363: 809-819, 2010.

26. Kim KB, Cabanillas ME, Lazar AJ, Williams MD, Sanders DL, Ilagan JL, Nolop K, Lee RJ and Sherman SI: Clinical responses to vemurafenib in patients with metastatic papillary thyroid cancer harboring BRAF(V600E) mutation. *Thyroid* 23: 1277-1283, 2013.
27. Abe Y, Matsumoto S, Kito K and Ueda N: Cloning and expression of a novel MAPKK-like protein kinase, lymphokine-activated killer T-cell-originated protein kinase, specifically expressed in the testis and activated lymphoid cells. *J Biol Chem* 275: 21525-21531, 2000.
28. Shih MC, Chen JY, Wu YC, Jan YH, Yang BM, Lu PJ, Cheng HC, Huang MS, Yang CJ, Hsiao M and Lai JM: TOPK/PBK promotes cell migration via modulation of the PI3K/PTEN/AKT pathway and is associated with poor prognosis in lung cancer. *Oncogene* 31: 2389-2400, 2012.
29. Park JH, Nishidate T, Nakamura Y and Katagiri T: Critical roles of T-LAK cell-originated protein kinase in cytokinesis. *Cancer Sci* 101: 403-411, 2010.
30. Xing M, Haugen BR and Schlumberger M: Progress in molecular-based management of differentiated thyroid cancer. *Lancet* 381: 1058-1069, 2013.
31. Treglia G, Aktolun C, Chiti A, Frangos S, Giovannella L, Hoffmann M, Iakovou I, Mihailovic J, Krause BJ, Langsteger W, *et al*: The 2015 Revised American Thyroid Association guidelines for the management of medullary thyroid carcinoma: The 'evidence-based' refusal to endorse them by EANM due to the 'not evidence-based' marginalization of the role of Nuclear Medicine. *Eur J Nucl Med Mol Imaging* 43: 1486-1490, 2016.
32. Matsuo Y, Park JH, Miyamoto T, Yamamoto S, Hisada S, Alachkar H and Nakamura Y: TOPK inhibitor induces complete tumor regression in xenograft models of human cancer through inhibition of cytokinesis. *Sci Transl Med* 6: 259ra145, 2014.
33. Lay JD, Hong CC, Huang JS, Yang YY, Pao CY, Liu CH, Lai YP, Lai GM, Chang AL, Su IJ and Chuang SE: Sulfasalazine suppresses drug resistance and invasiveness of lung adenocarcinoma cells expressing AXL. *Cancer Res* 67: 3878-3887, 2007.
34. Robe PA, Bentires-Alj M, Bonif M, Rogister B, Deprez M, Haddada H, Khac MT, Jolois O, Erkmen K, Merville MP, *et al*: In vitro and in vivo activity of the nuclear factor-kappaB inhibitor sulfasalazine in human glioblastomas. *Clin Cancer Res* 10: 5595-5603, 2004.
35. Yuan J, Gu K, He J and Sharma S: Preferential up-regulation of osteopontin in primary central nervous system lymphoma does not correlate with putative receptor CD44v6 or CD44H expression. *Hum Pathol* 44: 606-611, 2013.
36. Montgomery RM, Queiroz LS and Rogerio F: EGFR, p53, IDH-1 and MDM2 immunohistochemical analysis in glioblastoma: Therapeutic and prognostic correlation. *Arq Neuropsiquiatr* 73: 561-568, 2015.
37. Wienken CJ, Baaske P, Rothbauer U, Braun D and Duhr S: Protein-binding assays in biological liquids using microscale thermophoresis. *Nat Commun* 1: 100, 2010.
38. Jung SK, Lee KW, Byun S, Kang NJ, Lim SH, Heo YS, Bode AM, Bowden GT, Lee HJ and Dong Z: Myricetin suppresses UVB-induced skin cancer by targeting Fyn. *Cancer Res* 68: 6021-6029, 2008.
39. Irwin JJ, Sterling T, Mysinger MM, Bolstad ES and Coleman RG: ZINC: A free tool to discover chemistry for biology. *J Chem Inf Model* 52: 1757-1768, 2012.
40. Fiser A and Sali A: Modeller: Generation and refinement of homology-based protein structure models. *Method Enzymol* 374: 461-491, 2003.
41. Kirubakaran P, Karthikeyan M, Singh KhD, Nagamani S and Premkumar K: In silico structural and functional analysis of the human TOPK protein by structure modeling and molecular dynamics studies. *J Mol Model* 19: 407-419, 2013.
42. Abagyan R, Totrov M and Kuznetsov D: ICM-A new method for protein modeling and design: Applications to docking and structure prediction from the distorted native conformation. *J Computational Chemistry* 15: 488-506, 1994.
43. Liu Z, Hou P, Ji M, Guan H, Studeman K, Jensen K, Vasko V, El-Naggar AK and Xing M: Highly prevalent genetic alterations in receptor tyrosine kinases and phosphatidylinositol 3-kinase/akt and mitogen-activated protein kinase pathways in anaplastic and follicular thyroid cancers. *J Clin Endocrinol Metab* 93: 3106-3116, 2008.
44. Kunavisarut T: Diagnostic biomarkers of differentiated thyroid cancer. *Endocrine* 44: 616-622, 2013.
45. Wang CC, Friedman L, Kennedy GC, Wang H, Kebebew E, Steward DL, Zeiger MA, Westra WH, Wang Y, Khanafshar E, *et al*: A large multicenter correlation study of thyroid nodule cytopathology and histopathology. *Thyroid* 21: 243-251, 2011.
46. Yassa L, Cibas ES, Benson CB, Frates MC, Doubilet PM, Gawande AA, Moore FD Jr, Kim BW, Nosé V, Marqusee E, *et al*: Long-term assessment of a multidisciplinary approach to thyroid nodule diagnostic evaluation. *Cancer* 111: 508-516, 2007.
47. Ferraz C, Eßlinger M and Paschke R: Current state and future perspective of molecular diagnosis of fine-needle aspiration biopsy of thyroid nodules. *J Clin Endocr Metab* 96: 2016-2026, 2011.
48. Nikiforov YE, Steward DL, Robinson-Smith TM, Haugen BR, Klopfer JP, Zhu Z, Fagin JA, Falciglia M, Weber K and Nikiforova MN: Molecular testing for mutations in improving the fine-needle aspiration diagnosis of thyroid nodules. *J Clin Endocrinol Metab* 94: 2092-2098, 2009.
49. Eßlinger M and Paschke R: Molecular fine-needle aspiration biopsy diagnosis of thyroid nodules by tumor specific mutations and gene expression patterns. *Mol Cell Endocrinol* 322: 29-37, 2010.
50. Rao SN, Zafereo M, Dadu R, Busaidy NL, Hess K, Cote GJ, Williams MD, William WN, Sandulache V, Gross N, *et al*: Patterns of treatment failure in anaplastic thyroid carcinoma. *Thyroid* 27: 672-681, 2017.
51. Vasko VV, Gaudart J, Allasia C, Savchenko V, Di Cristofaro J, Saji M, Ringel MD and De Micco C: Thyroid follicular adenomas may display features of follicular carcinoma and follicular variant of papillary carcinoma. *Eur J Endocrinol* 151: 779-786, 2004.
52. Simons-Evelyn M, Bailey-Dell K, Toretsky JA, Ross DD, Fenton R, Kalvakolanu D and Rapoport AP: PBK/TOPK is a novel mitotic kinase which is upregulated in Burkitt's lymphoma and other highly proliferative malignant cells. *Blood Cells Mol Dis* 27: 825-829, 2001.
53. Park JH, Lin ML, Nishidate T, Nakamura Y and Katagiri T: PDZ-binding kinase/T-LAK cell-originated protein kinase, a putative cancer/testis antigen with an oncogenic activity in breast cancer. *Cancer Res* 66: 9186-9195, 2006.
54. Zhu F, Zykova TA, Kang BS, Wang Z, Ebeling MC, Abe Y, Ma WY, Bode AM and Dong Z: Bidirectional signals transduced by TOPK-ERK interaction increase tumorigenesis of HCT116 colorectal cancer cells. *Gastroenterology* 133: 219-231, 2007.
55. Brown-Clay JD, Shenoy DN, Timofeeva O, Kallakury BV, Nandi AK and Banerjee PP: PBK/TOPK enhances aggressive phenotype in prostate cancer via b-catenin-TCF/LEF-mediated matrix metalloproteinases production and invasion. *Oncotarget* 6: 15594-15609, 2015.
56. Sun H, Zhang L, Shi C, Hu P, Yan W, Wang Z, Duan Q, Lu F, Qin L, Lu T, *et al*: TOPK is highly expressed in circulating tumor cells, enabling metastasis of prostate cancer. *Oncotarget* 6: 12392-12404, 2015.
57. Kim DJ, Li Y, Reddy K, Lee MH, Kim MO, Cho YY, Lee SY, Kim JE, Bode AM and Dong Z: Novel TOPK inhibitor HI-TOPK-032 effectively suppresses colon cancer growth. *Cancer Res* 72: 3060-3068, 2012.
58. Novel molecule targets cytokinesis. *Cancer Discov* 5: OF8, 2015.
59. Tobinick EL: The value of drug repositioning in the current pharmaceutical market. *Drug News Perspect* 22: 119-125, 2009.
60. Liu Y, Liu H, Cao H, Song B, Zhang W and Zhang W: PBK/TOPK mediates promyelocyte proliferation via Nrf2-regulated cell cycle progression and apoptosis. *Oncol Rep* 34: 3288-3296, 2015.
61. Shinde SR, Gangula NR, Kavela S, Pandey V and Maddika S: TOPK and PTEN participate in CHFR mediated mitotic checkpoint. *Cell Signal* 25: 2511-2517, 2013.



This work is licensed under a Creative Commons Attribution-NonCommercial-NoDerivatives 4.0 International (CC BY-NC-ND 4.0) License.